Measuring 8- to 250-ps Short Pulses Using a High-Speed Streak Camera on Kilojoule, Petawatt-Class Laser Systems

Introduction

Optical streak cameras have been used as the primary diagnostic for a variety of laser and target experiments. OMEGA EP[1] uses a high-speed optical streak camera comprising a P820 streak tube[2] in a ROSS (Rochester Optical Streak System)[3–5] to measure the pulse shape for pulse durations ranging from 8 to 250 ps. A small percentage (0.7%) of the main laser beam (370 mm × 370 mm) is picked off by a full-size diagnostic mirror, demagnified to a size of 65 mm × 65 mm by a down-collimator inside the grating compressor chamber (GCC), and transported to the short-pulse diagnostic package (SPDP) residing outside the GCC. This diagnostic beam is further demagnified to 4 mm × 4 mm by three stages of down-collimators inside the SPDP (65 mm × 65 mm to 25 mm × 25 mm, to 12 mm × 12 mm, and, finally, to 4 mm × 4 mm). In the initial configuration, the 4-mm × 4-mm beam was focused onto the input slit of the ROSS by a cylindrical lens. The streak image of the line focus provides the temporal profile and the spatial profile in one direction of the laser beam. The focusing of a laser beam with aberration [approximately 0.5-λ rms (root mean square), λ = 1053 nm] by a cylindrical lens produces multiple local hot spots within the focal line. Because of shot-to-shot focal-spot pointing and structure variations, these hot spots move across the slit in both the space and time directions, leading to distorted pulse-shape measurements. Moreover, interactions among the photoelectrons transiting in the streak tube cause the electrons to repel each other (space-charge broadening).[6] This effect is particularly pronounced for shorter pulses, leading to an artificially broadened pulse measurement. The space-charge broadening is further exacerbated by the hot spots imaged onto the photocathode. The signal's sensitivity to far-field–based coupling and the space-charge broadening make it very challenging to operate a streak camera during short-pulse laser operations. The initial shot-to-shot streak measurements are found to exhibit a large signal variation (5:1 is typical), making it operationally impractical to accurately control space-charge–induced pulse broadening and to operate the streak camera within the traditionally defined dynamic range of less than 20% broadening.[6]

We report a beam-homogenizing method that uses an anamorphic diffuser to provide significantly more uniform illumination on the photocathode of a streak camera as compared with the conventional cylindrical-lens coupling approach, therefore increasing the signal-to-noise ratio and the ability to conduct a global space-charge–broadening calibration. A method to calibrate space-charge–induced pulse broadening of streak-camera measurements is described and validated by modeling and experiments.

Anamorphic Diffuser for Uniform Photocathode Illumination

Figure 133.54(a) illustrates a typical streak image of a 230-ps laser pulse obtained with the cylindrical-lens–coupling approach. Figures 133.54(b) and 133.54(c) show the corresponding spatial and temporal profiles, respectively. The hot spots typically induce an undesired 5-to-1 spatial modulation. As shown in Fig. 133.54(c), the pulse shape is also somewhat distorted into a tilted top by the hot spots present during the first half of the pulse. The spatial-profile variation at different times also indicates that the streak image is sensitive to the far-field structure and pointing changes. A new coupling scheme is required to provide more-uniform streak images, higher signal-to-noise ratios, and less sensitivity to focal-spot structure and pointing changes.

An anamorphic-diffuser–based coupler has been developed to provide more-uniform streak images and to increase the signal-to-noise ratio. Figures 133.55(a) and 133.55(b) show the principle of the new coupling approach: it consists of an anamorphic diffuser followed by a spherical focusing lens. The divergence angles of the anamorphic diffuser are 10° and 0.4° along and across the ROSS slit (corresponding to the spatial and temporal directions), respectively. A 12-mm × 12-mm collimated beam is transmitted through the diffuser and diverges into a 10° × 0.4° solid angle. The focusing lens, having a 35-mm focal length, transfers the common angle from the diffuser to the same location on the focal plane, forming a focal line. All the rays with the same angle on the object plane contribute to

the energy collected at a particular location on the focal plane; therefore, any hot spot in the incoming beam will be averaged out at the image plane.

The spatial profile of this diffuser-based coupler was measured with a continuous-wave (cw) laser at a 675-nm wavelength. The profiles along the spatial and temporal directions are shown in Figs. 133.55(c) and 133.55(d), respectively. The full-width-at-half-maximum (FWHM) spot sizes are 270 μm and 6.1 mm across and along the slit, respectively. The measured coupling efficiency through a 100-μm slit was 20%.

The diffuser coupler was tested with a ROSS on a pulsed laser system. Figures 133.56(a)–133.56(c) show the measured

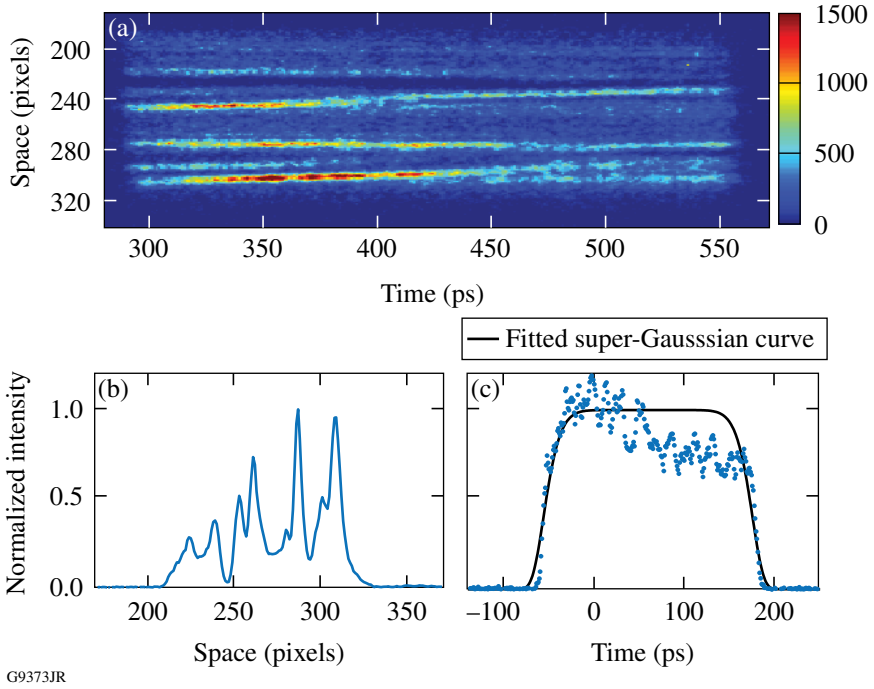

Figure 133.54
(a) Streak image with a cylindrical lens coupling; (b) spatial profile showing modulation from the hot spots; (c) temporal profile distorted by the hot spots.

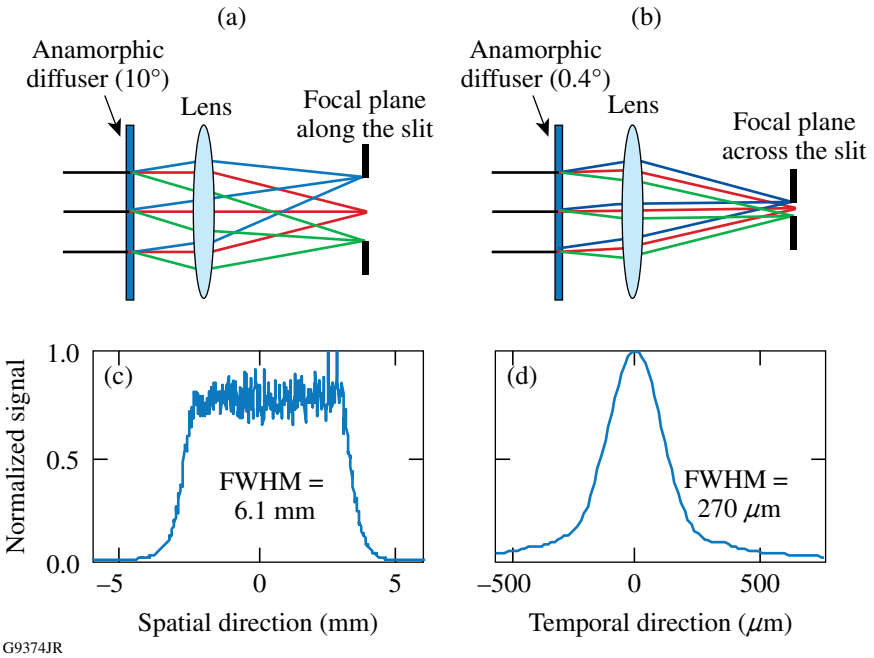

Figure 133.55
[(a),(c)] A 10° divergence angle in the spatial direction achieved a 6.1-mm-long focal line along the slit. [(b),(d)] A 0.4° divergence angle in the temporal direction achieved a 270-μm-wide focal line across the slit.

streak image and spatial and temporal profiles of a 180-ps (FWHM) laser pulse. Compared to the cylindrical-lens coupling results shown in Fig. 133.54, the anamorphic-diffuser–based coupling provides a more-uniform photocathode illumination; the spatial modulation is less than 2:1, down from 5:1 for the cylindrical-coupling approach. Figure 133.57 illustrates that the temporal distortions induced by the hot spots in region of interest #2 (ROI2) [Fig. 133.57(a)] with the cylindrical lens coupling were eliminated through the more-uniform illumination [Fig. 133.57(b)] on the photocathode with the 10° × 0.4° diffuser [comparing Figs. 133.57(a), 133.57(c) and 133.57(b), 133.57(d)]. Therefore, consistent temporal profiles are achieved

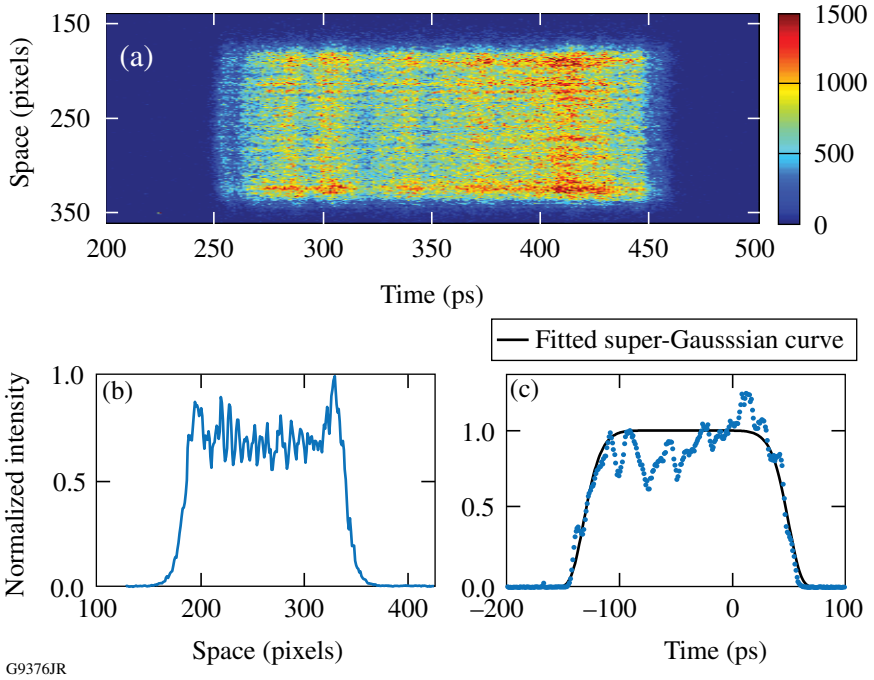

Figure 133.56
(a) A streak image obtained with the 10° × 0.4° diffuser; (b) spatial profile; (c) temporal profile.

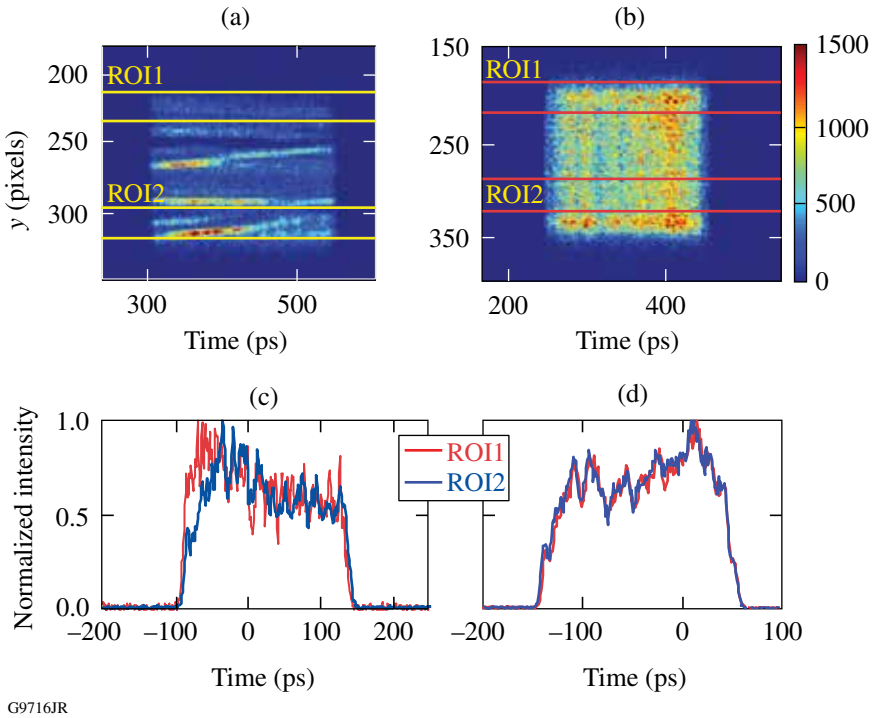

Figure 133.57
[(a),(c)] Streak image and temporal profiles obtained through a cylindrical lens. Temporal profiles were distorted by the hot spots in ROI2. [(b),(d)] Streak image and temporal profiles obtained through a 10° × 0.4° diffuser. Temporal profiles are consistent across the spatial direction.

across the spatial direction. A higher signal-to-noise ratio can be achieved by averaging across the spatial direction without compromising the pulse-shape measurement.

The maximum optical-path difference (OPD) of the rays traveling from the diffuser to the focal plane was investigated in *OSLO*®, and induced pulse broadening was found to be less than 0.5 ps (140 λ, λ = 1053 nm). The impulse response of the ROSS and diffuser-coupler system was measured with a subpicosecond pulse to verify that diffuser-induced pulse broadening was minimal. The measured impulse response width remained at 3 ps (FWHM, shown in Fig. 133.58), narrow enough to measure 10-ps pulses.

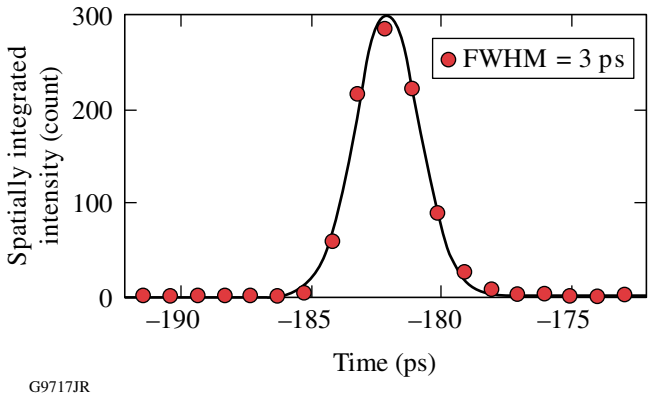

Figure 133.58
Impulse response of the streak camera using the 10° × 0.4° diffuser with a 3-ps FWHM.

Characterization of Space-Charge–Broadening Effects

Maintaining the dynamic range of a streak camera requires that the input signal to the photocathode be controllable under a certain level and stable from shot to shot. However, the large 5-to-1, shot-to-shot streak signal variation makes it difficult to control the space-charge–induced broadening effect. Therefore, the traditionally defined dynamic range is operationally impractical to achieve; the pulse width broadens with an increasing total number of electrons per pulse.

The spatial averaging produced by the diffuser eliminates the local hot spots imaged to the photocathode and subsequently simplifies the space-charge mechanism so that pulse broadening depends on the total current in the tube, rather than on local variations in intensity. As a result, a global space-charge analysis can be used to determine the amount of broadening from the total signal, integrated in space and time.

A method to calibrate space-charge–induced pulse broadening has been developed and validated on OMEGA EP. The input energy to the slit of the ROSS was varied to obtain a series of broadened pulses for each stretcher position. The true pulse width was determined by a linear regression between the measured pulse width and the total pixel values in an analog-to-digital units (ADU's) measured by the ultrafast ROSS charge-coupled device (CCD). The offset at zero ADU represents the true pulse width without space-charge broadening.

Rather than using a 10° × 0.4° diffuser that provided only 20% coupling efficiency, a 10° × 0° diffuser with 75% coupling efficiency was used to provide sufficient energy for a ROSS on OMEGA EP to characterize the space-charge effects on streak measurements of short pulses with various lengths and shapes. Characterization traces were measured for stretcher positions of 16 mm, 40 mm, and 80 mm (relative to the position corresponding to a best-compression pulse width of approximately 1 ps). With the full front-end spectrum, these stretcher positions produce approximately square pulses with FWHM's of 23 ps, 58 ps, and 120 ps, respectively, as predicted by a system model. When the beamline amplifiers are fired, spectral gain narrowing produces approximately Gaussian pulses with widths of 10 ps, 25 ps, and 50 ps for these stretcher positions. Figure 133.59 demonstrates that the pulse width linearly increases with the total signal on the photocathode. In the absence of gain narrowing, for stretcher positions of 16 mm, 40 mm, and 80 mm, the regressed true pulse widths are 21.1 ps, 55.7 ps, and 113.7 ps, respectively. The corresponding 95%

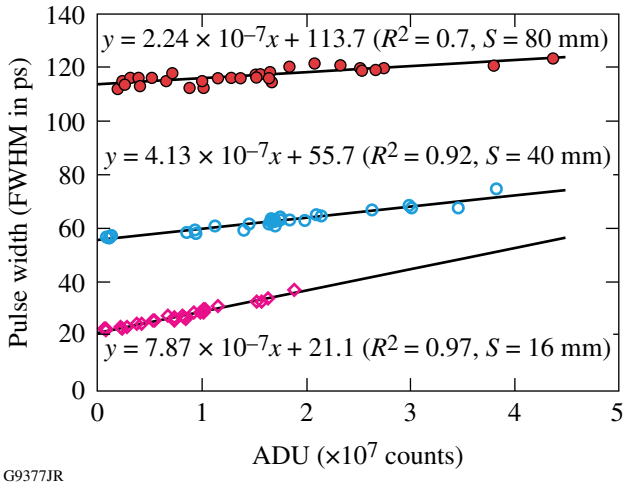

Figure 133.59
Space-charge–broadening calibration for stretcher positions of S = 16 mm, S = 40 mm, and S = 80 mm.

confidence intervals are [20.6 ps, 21.7 ps]; [54.8 ps, 56.7 ps]; and [112.7 ps, 114.7 ps]. The slopes obtained from linear regressions between the measured pulse width and photocathode signal at each stretcher position reveal that the magnitude of the space-charge–broadening effect depends on the stretcher position, i.e., the pulse width to be measured. The shorter the pulse to be measured, the larger the slope, and the more pronounced the space-charge–broadening effects.

Figure 133.60 shows the inverse relation between space-charge–induced pulse broadening (slope) and pulse width (offset) for both square and Gaussian pulses. For the limited number of measurements, the space-charge–broadening effect is comparable for these two pulse shapes, although the electron density at the edges of a Gaussian pulse is smaller than that of a square pulse. One would expect the effect on the former is less than that on the latter because a Gaussian pulse shape distorts to a super-Gaussian and to a square pulse shape with the increasing energy to the input slit.[7]

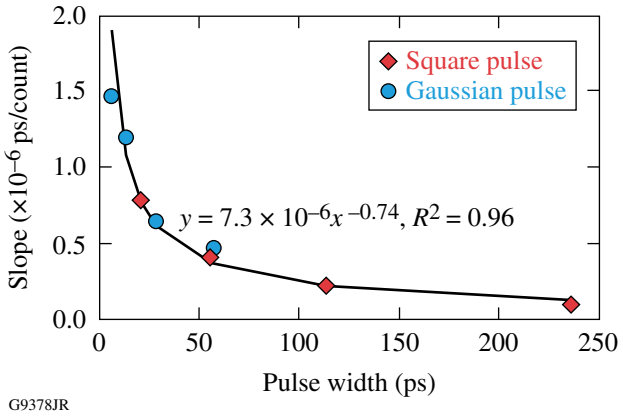

Figure 133.60
Inverse relation between space-charge broadening and pulse width.

During laser operations, the slope of each calibration trace, in conjunction with the streak-image signal level and measured pulse width, can be used to determine the true pulse width, removing space-charge–broadening effects.

The inferred pulses are compared to the results from an *EPSys* model[8] that predicts the pulse shape from the measured spectrum, the stretcher and compressor angles, and the stretcher slant distance. The pulse widths determined using the two methods show a systematic error of 5% (Fig. 133.61). Figure 133.62(a) shows a uniform streak image obtained on a high-energy shot. Figure 133.62(b) illustrates that the measured pulse shape, at a low input energy level to minimize space-charge broadening, agrees with the *EPSys*-predicted pulse shape.

To validate the accuracy of the space-charge–broadening calibration method, a <10-ps inferred pulse from the streak-camera measurements was compared to the measurements from

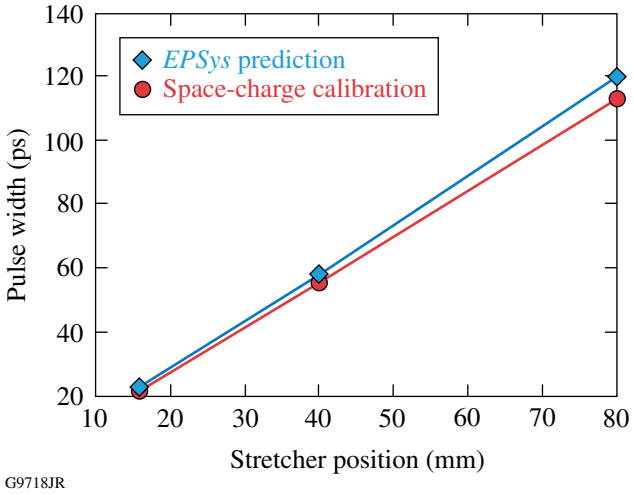

Figure 133.61
Comparison of results from space-charge–broadening calibration and *EPSys* prediction.

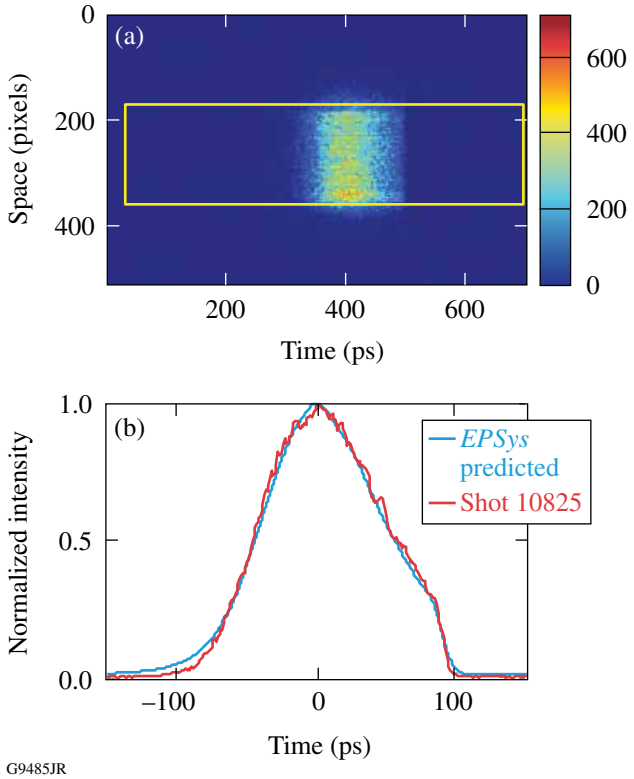

Figure 133.62
(a) Uniform streak image achieved on high-energy laser shots; (b) Measured pulse shape and model prediction.

a scanning autocorrelator (suitable for pulses ranging from 0.2 to 20 ps). Figure 133.63(a) shows the streak-camera data. The pulse width (FWHM), after a space-charge–broadening calibration was applied, was 8.7 ps±0.5 ps. Figure 133.63(b) shows three consecutive autocorrelation measurements with an averaged FWHM of 11.5 ps and a standard deviation of 0.1 ps. By applying a decorrelation factor of 1.36 (the ratio of the width of the autocorrelation of the pulse predicted by *EPsys* to the width of the pulse itself), the pulse width determined from the scanning autocorrelator was 8.5 ps, which agrees with the space-charge–broadening-calibrated measurement of 8.7 ps by the ultrafast ROSS.

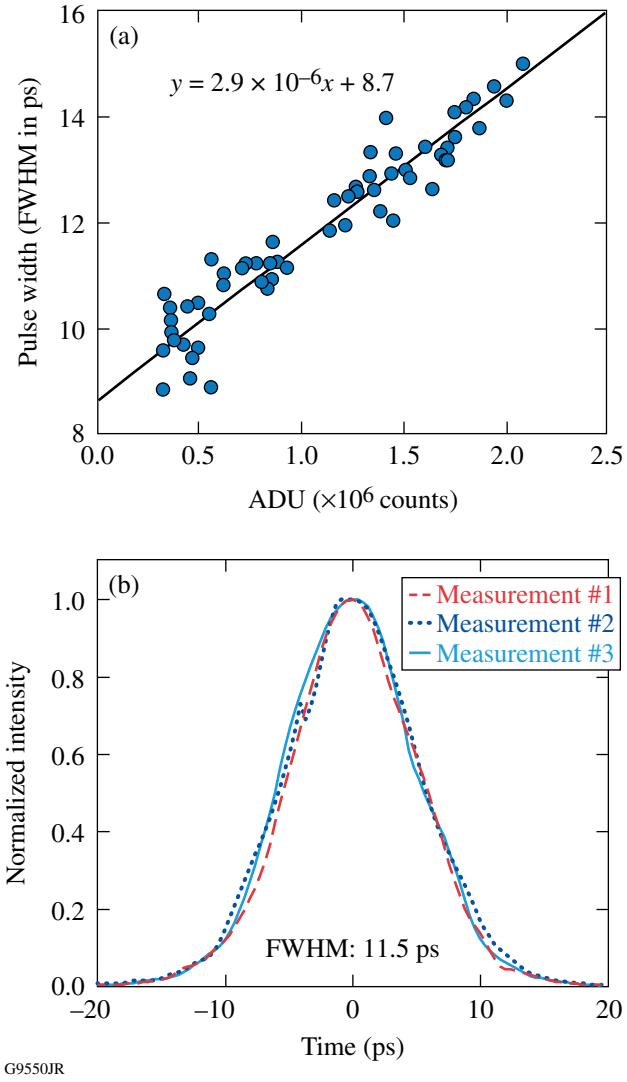

Figure 133.63
(a) Space-charge–broadening-calibrated pulse measurement (FWHM = 8.7 ps). (b) Three autocorrelation measurements leading to a pulse FWHM of 8.5 ps using a decorrelation factor of 1.36 obtained by modeling.

Conclusions

The insertion of an anamorphic-diffuser coupler provides more-uniform photocathode illumination, less sensitivity to focal-spot pointing and structure changes, and improved space-charge–broadening characterization, resulting in improved pulse-measurement accuracy. A linear regression method was developed to calibrate space-charge–broadening effects. By increasing the effective dynamic range and reducing the sensitivity to wavefront errors, the space-charge–broadening calibration method, in conjunction with the anamorphic diffuser coupler, allows one to more easily operate a streak camera and obtain more-accurate pulse measurements in the 8- to 250-ps range on OMEGA EP. This approach is well suited for other short-pulse laser systems.

ACKNOWLEDGMENT

This work was supported by the U.S. Department of Energy Office of Inertial Confinement Fusion under Cooperative Agreement No. DE-FC52-08NA28302, the University of Rochester, and the New York State Energy Research and Development Authority. The support of DOE does not constitute an endorsement by DOE of the views expressed in this article. The authors thank M. Millecchia and A. Kalb for their support on the anamorphic-diffuser–based coupler testing.

REFERENCES

1. J. H. Kelly, L. J. Waxer, V. Bagnoud, I. A. Begishev, J. Bromage, B. E. Kruschwitz, T. J. Kessler, S. J. Loucks, D. N. Maywar, R. L. McCrory, D. D. Meyerhofer, S. F. B. Morse, J. B. Oliver, A. L. Rigatti, A. W. Schmid, C. Stoeckl, S. Dalton, L. Folnsbee, M. J. Guardalben, R. Jungquist, J. Puth, M. J. Shoup III, D. Weiner, and J. D. Zuegel, J. Phys. IV France **133**, 75 (2006).

2. PHOTONIS, 19106 Brive, France.

3. W. R. Donaldson, R. Boni, R. L. Keck, and P. A. Jaanimagi, Rev. Sci. Instrum. **73**, 2606 (2002).

4. R. A. Lerche, J. W. McDonald, R. L. Griffith, G. Vergel de Dios, D. S. Andrews, A. W. Huey, P. M. Bell, O. L. Landen, P. A. Jaanimagi, and R. Boni, Rev. Sci. Instrum. **75**, 4042 (2004).

5. Sydor Instruments, LLC, Rochester, NY 14624.

6. D. J. Bradley *et al.*, Rev. Sci. Instrum. **49**, 215 (1978).

7. X. Wang *et al.*, Rev. Sci. Instrum. **80**, 013902 (2009).

8. *Final Proposal for Renewal Award for Cooperative Agreement DE-FC52-92SF-19460*, Between the U.S. Department of Energy and the Laboratory for Laser Energetics of the University of Rochester, Part 1: Technical Program (Rochester, NY, 2007), p. 2.245.